

# Computed Tomography Studies of Lung Mechanics

Brett A. Simon, Gary E. Christensen, Daniel A. Low, and Joseph M. Reinhardt

Department of Anesthesiology/Critical Care Medicine and Department of Medicine, Johns Hopkins University, Baltimore, Maryland; Departments of Electrical and Computer Engineering and Biomedical Engineering, University of Iowa, Iowa City, Iowa; and Department of Radiation Oncology, Mallinckrodt Institute of Radiology, Washington University School of Medicine, St. Louis, Missouri

The study of lung mechanics has progressed from global descriptions of lung pressure and volume relationships to the high-resolution, three-dimensional, quantitative measurement of dynamic regional mechanical properties and displacements. X-ray computed tomography (CT) imaging is ideally suited to the study of regional lung mechanics in intact subjects because of its high spatial and temporal resolution, correlation of functional data with anatomic detail, increasing volumetric data acquisition, and the unique relationship between CT density and lung air content. This review presents an overview of CT measurement principles and limitations for the study of regional mechanics, reviews some of the early work that set the stage for modern imaging approaches and impacted the understanding and management of patients with acute lung injury, and presents evolving novel approaches for the analysis and application of dynamic volumetric lung image data.

**Keywords:** computed tomography; mathematical modeling; physiology

The phenomena covered by the word "respiration" are very diverse. When a person is seen to breathe, what is observed is a movement of the chest and abdomen by which air is alternately drawn into his lungs and again expelled. This constitutes the mechanical aspect of respiration.

—August Krogh, 1941

In the 60-odd years since A. Krogh (1) opened his treatise on the comparative physiology of respiration with these words, an enormous amount of work has explored the relationship between lung expansion or deformation and the forces that drive such changes. Most recently, advances in imaging techniques have extended the study of lung mechanical behavior to the regional level, and currently evolving technologies permit the three-dimensional characterization of dynamic lung volume changes in intact subjects. X-ray computed tomography (CT), because of its speed, widespread availability, high-resolution anatomic visualization, and unique ability to quantify regional air and tissue volumes, provides a particularly powerful tool for the noninvasive measurement of lung mechanics in experimental models as well as human subjects. This review presents relevant CT measurement principles for regional mechanics, presents examples of static and dynamic approaches to lung mechanics, and emphasizes some exciting and promising new high-resolution, vol-

umetric methods for characterizing lung mechanical properties throughout the whole lung.

In the simplest sense, lung mechanics describes the relationship between the expansion of the lung and the forces driving that expansion, the most basic measure being lung compliance or the ratio between volume and pressure change, but also includes airways and airflow, lung tissue material properties, interdependence, and chest wall and diaphragm properties and interactions. Limited initially to measuring global gas entry into the lung and total lung volumes, investigators began to explore indirect methods such as lung frequency response (2) or exhaled gas concentration profiles (3) to probe the distribution of this inspired gas within the lung and the effect of regional mechanical properties. Invasive techniques, including the retrograde catheter (4, 5), alveolar capsule (6), and implanted radiopaque markers (7), added greatly to our understanding of regional lung function but obviously could not be applied in human disease. The use of noninvasive imaging methods, initially with low-resolution planar detectors and radioactive tracer gases (8) and then by tomographic methods of increasing resolution and volumetric data acquisition (9–13) (again, enhanced by coupling to models of distributed lung function [14]), now provides an unprecedented capability for understanding regional lung mechanical function in general as well as in individual patients.

## CT MEASUREMENT PRINCIPLES

Although modern CT scanners have greatly improved the speed, resolution, and (with multidetector hardware) volume of tissue simultaneously imaged, the two quantities measured remain, simply density and volume. Density is measured in the Hounsfield unit (HU) scale, defined (approximately) as  $-1,000$  HU for air,  $0$  HU for water, and  $1,000$  HU for bone. If one considers that the lung is composed essentially of two "materials" of known density: air, at  $-1,000$  HU and "tissue" (including blood, cells, water, etc.) at  $0$  HU, then the density in Hounsfield units may be converted directly into the air and tissue content of the region of interest (ROI) imaged. For example, an ROI with density of  $-600$  HU contains an average of 60% air and 40% "tissue." Importantly, the exact Hounsfield unit values for air and tissue vary over time and between scanners, and thus best results are obtained by measuring actual air and tissue values from specific image sets and calibrating the results on the basis of those reference values (15, 16). Volume is the product of the in-plane cross-sectional area of the ROI and the slice thickness, summed over all the slices spanning the ROI. The absolute volumes of air or tissue in an ROI may then be obtained from the region volume multiplied by the fraction of air or tissue. Because modern scanners have high spatial resolution, the limitation in accurately defining lung volumes is generally due to difficulties in defining the edges or boundaries of the tissue ("segmentation"), which may be blurred because of motion artifact, small density differences from the adjacent tissue, or partial volume effects. Note that this analysis requires that the lung be composed of elements with one of two densities; the introduction of a third density compartment (such as an intravascular contrast agent) violates

(Received in original form July 30, 2005; accepted in final form September 19, 2005)

Supported by National Institutes of Health grants HL64368, HL073994, CA976679, and EB004126; Department of Defense DAMD17-02-1-0732; and National Science Foundation 0092758.

Correspondence and requests for reprints should be addressed to Brett A. Simon, M.D., Ph.D., Department of Anesthesiology, Tower 711, Johns Hopkins Hospital, 600 North Wolfe Street, Baltimore, MD 21287-8711. E-mail: bsimon@jhmi.edu

The color figures for this article are on pp. 506–507.

Proc Am Thorac Soc Vol 2, pp 517–521, 2005

DOI: 10.1513/pats.200507-076DS

Internet address: www.atsjournals.org

this assumption and makes calculation of regional aeration and partitioning of air and tissue volumes more complex because the system is no longer described by two equations in two unknowns. In some cases, such as with contrast injection, the volume of the “third” compartment may be estimated from the difference between pre- and postinjection images and the air and tissue compartment volumes may then be computed (17).

CT-based measures of lung mechanical function rely on one of two principles, both of which are discussed in detail below. Most commonly, regional mechanics are defined by relating regional lung air volume change, derived from CT total volume and density changes as described above, to estimates or measurements of distending or inflation pressure. This approach has been used successfully to provide insight into the pathophysiology of acute lung injury, particularly with respect to recruitment and ventilator management (18–22). However, as pointed out in a Critical Care Perspective (23), CT analysis based on density cannot detect volume changes of lung units that are flooded and that may expand as more fluid enters. Furthermore, as the mean density within an ROI falls because of gas inflow, CT cannot distinguish how that gas distributes at the alveolar level, that is, whether some alveoli inflate to a greater extent at the expense of others within the region.

A second, newer approach uses image registration, in which the anatomic and structural detail in image sets are used to generate a three-dimensional mapping of the lung from one state to another (24, 25), as from end expiration to end inspiration. The deformation description obtained can be used to quantitate global and regional volume changes as well as local volumetric and directional strains (25, 26), as detailed below.

Finally, whereas early studies were typically limited to imaging during constant airway pressure breathholds, modern CT scanners have scan apertures as low as 100 to 500 ms, permitting gated imaging during continuous respiration to stop motion. Although the volume coverage of multislice scanners is increasing every year, to capture volumetric data it is necessary either to repeat the “prospective” gated imaging protocol (i.e., image acquisition gated to specific points in the ongoing respiratory cycle) at multiple table positions or to apply “retrospective” gating techniques. In retrospective gating, initially developed for cardiac imaging (27), a slow helical scan is performed with continuous image data acquisition during steady breathing along with a signal synchronous with the respiratory cycle, such that all table locations are imaged at all points of the respiratory cycle (28, 29). The images are then later (retrospectively) reconstructed in three dimensions at the desired time points in the cycle, giving true dynamic, volumetric image data. Although retrospective gating currently has the disadvantage of high radiation exposure, the ability to image the lung at multiple points in the respiratory cycle during physiologic breathing will be important in extending our understanding of *in vivo* lung mechanical function from static to dynamic, steady-state conditions.

## ASSUMPTIONS AND LIMITATIONS

Although imaging permits measurement of regional volume change in the lung, it is not possible to noninvasively measure regional pressure changes; thus, descriptions of regional mechanics require assumptions about the local pressure distributions. These assumptions become more problematic as conditions vary from static to dynamic and as regional heterogeneity increases. Furthermore, the lung responds to changes in transpulmonary pressure (alveolar–intrapleural) (30), but because of difficulties in measuring intrapleural pressure many descriptions of lung mechanics in human subjects refer to respiratory system (lung plus chest wall) properties. Even if a measure of average pleural

pressure, such as from an esophageal balloon, were available, the local intrapleural pressures required for a true measure of regional lung mechanics would not be. On the other hand, one could argue that respiratory system mechanics, which include the effect of the chest wall and abdomen, are the most relevant for management of patient issues because this approach reflects the actual *in situ* patient condition and there are limited clinical interventions that separate chest wall and lung effects.

A second important caveat with respect to CT imaging relates to the use of slice versus volumetric imaging. The lung moves relative to the image plane during tidal breathing, and thus repeat imaging at the same table location during changes in lung volume can result in the quantitative comparison of measurements made in anatomically different lung regions. The high-resolution anatomic detail available in CT images frequently permits the manual matching of distinct ROI between different image sets (31), but this is possible only if multiple slices covering the moving ROI are obtained. However, unless three-dimensional image registration methods are used to ensure that the same tissue elements are included in all tracked regions (24), absolute volumes computed from slice data are subject to significant registration errors. Calculations based on density measurements, in contrast, are more robust because average density is less sensitive to small errors in boundary registration. Several important studies have highlighted the potential errors associated with under-sampling or single-slice analysis (32, 33). Alternatively, whole lung or lobar analysis permits the use of conservation of mass principles to measure changes in absolute air or tissue volumes. Lobar segmentation and analysis revealed important differences in the involvement and mechanical behavior of upper versus lower lobes in patients with acute lung injury (34), a finding that was not evident when the same data were analyzed with the typical global Cartesian axes because of averaging across lobes.

## EARLY STUDIES OF REGIONAL LUNG MECHANICS

Two important early imaging approaches to regional lung mechanics originated at the Mayo Clinic (Rochester, MN), beginning in the late 1970s. Using metal parenchymal markers implanted in animals and a biplane X-ray cine system that tracked the marker positions during spontaneous and controlled ventilation, a series of landmark studies was performed that examined regional lung expansion under a variety of conditions. Comparing results in intact animals as well as excised lungs, these studies demonstrated differences in the distribution of lung expansion between prone and supine positioning (7), the uniformity of expansion within lobes and the motion of lobes relative to each other within the chest (7), and the importance of chest wall–lung interactions in determining regional lung expansion and mechanical strain (35–37). Subsequent applications of this method examined the heterogeneity of bronchoconstriction (38), regional diaphragm function (39), and most recently the controversy over flooding versus collapse in acute lung injury (40, 41). At about the same time, the dynamic spatial reconstructor, a predecessor of modern volumetric CT scanners, was built (42). Using an array of rotating X-ray sources and detectors, the dynamic spatial reconstructor could image a 21.5-cm cylindrical volume at 60 times per second to determine detailed *in vivo* structure–function relationships of the heart and lungs. This device was used to establish some of the fundamental relationships between lung density and volume changes, the interactions of the chest wall and regional lung expansion, and, again, the effect of body orientation on regional lung air content (43, 44). The mechanical and physiological relationships described by these basic studies remain benchmarks for the evaluation of current and future technologies.

## CT STUDIES OF AERATION DISTRIBUTION IN ACUTE LUNG INJURY

One of the most important contributions of CT imaging and lung mechanics to our understanding of the pathophysiology of human disease and consequent management is with respect to acute lung injury (ALI) (21, 45). The pioneering CT studies of Gattinoni and colleagues changed the prevailing view of ALI from that of a diffuse process, as evidenced from the relatively uniformly involved chest X-ray, to one in which the lung was heterogeneously involved. They showed that there were significant regional differences in lung aeration and recruitment behavior with tidal volume and positive end-expiratory pressure, and that these differences in regional parenchymal mechanical properties helped determine whether the local response to different management strategies was beneficial or potentially injurious. Although initial patient studies were limited by radiation exposure and slow imaging technology to a single or a few representative slices (18, 20), the basic principles relating regional density to regional aeration and partitioning air and tissues volumes were applied in a series of elegant studies of critically ill patients. Regional aeration patterns from CT data were used to shed light on the distinct shape of the whole lung pressure–volume curve in patients with ALI (19), and a classification scheme for different types of ALI based on CT and other characteristics with different therapeutic and prognostic features has been proposed (46, 47). Subsequent studies using high-speed scanning during brief breathholds have examined whole lung and lobar changes in lung air and tissue volumes (34, 48, 49), and have further emphasized the regional heterogeneity of the disease process and the importance of whole lung imaging for accurate assessment of regional behavior.

## THREE-DIMENSIONAL IMAGE REGISTRATION TECHNIQUES

Image registration is the alignment of three-dimensional image sets on the basis of common anatomic landmarks or other image features such as intensity patterns or boundaries (Figure 1 [p. 506]). These computer-based analyses allow the mapping of lung regions between image sets, whether acquired at different points in time or under different conditions (such as inflation), and also permit the comparison of individuals with other subjects or normal “standards” (24). Although this process was developed for the purpose of tracking changes in a patient’s condition (such as a nodule or mass) over time or for allowing quantitative comparison of individual images with a standard (24), it has important implications for the study of regional lung pathophysiology. First, it provides a mechanism for an accurate quantitative comparison of a three-dimensional ROI between image sets, unaffected by lung motion, expansion, and subject orientation in the scanner. In this mode, the boundaries of a three-dimensional ROI are mapped onto each image set and quantitative measures (mean density, density histogram, and volume) are determined. Second, the mathematical transform that describes the mapping of the lung from one volume to another also allows the voxel-by-voxel calculation of the local lung expansion or contraction as well as directional strains (26). Thus, given a pair of volumetric image sets from the same lung, a three-dimensional image may be created whose values (or colors) represent the local lung expansion or contraction between the two states (Figure 2 [p. 507]). When combined with evolving dynamic image acquisition techniques, this approach promises to provide new insights into important questions in lung mechanics such as regional interdependence, airway–parenchymal interactions, and parallel inhomogeneity, and possibly address the issue of regional flooding versus collapse in ALI raised

by Hubmayr (23) by simultaneously measuring local deformation and density change.

There are many general methodologies for three-dimensional image registration (50). One of the simplest methods is the optical flow method. This algorithm follows the distribution of apparent velocities of movement in brightness patterns in a set of images (51). It has been adapted for use in static breathhold lung CT images to monitor nodules and disease progression over time (52) and for radiation therapy treatment planning (25, 53). A second approach generates a three-dimensional warping function by aligning landmarks or other image features and then deforming the structure to minimize the differences in these parameters. Simpler approaches use manually identified landmarks in both image sets (54, 55), but this approach is extremely labor intensive. More advanced image registration approaches use combined image intensities and landmark information to determine correspondences. One such approach is the small-deformation inverse consistent linear elastic (SICLE) image registration technique (56–58). This approach assumes that the shape change that occurs over a short interval of time can be described by a small-deformation linear elastic model. This algorithm also estimates better correspondences by jointly estimating the forward and reverse transformations between two images while minimizing the inverse consistency registration error (58) between the forward and reverse transformations.

Once the image registration is determined, then the local tissue deformation (expansion or contraction) can be quantified from the log-Jacobian of the deformation field (26). This is illustrated in Figure 2 (p. 507), from a pilot study of patients with lung tumors in which a series of multislice CT images was acquired every 0.75 s during quiet breathing for three breathing cycles, repeated at different table positions to cover the entire lung. Spirometry (Figure 2, II) was used to measure whole lung tidal volume and to correlate the imaging with the respiratory cycle. SICLE image registration (58) was used to nonrigidly register adjacent 12-slice temporal image volumes. Figure 2 shows the midlung slice from the registration and is color-coded such that orange–red represents lung expansion from the first to the second volume, and blue–magenta represents contraction. Figure 2, III, demonstrates an excellent correlation between the volume change measured by spirometry and the mean log-Jacobian for the entire lung. The data show a somewhat unexpected dissynchrony between lung regions. For example, during exhalation from points E to F to G, the majority of the lung shows volume contraction, but there are regions in the dependent periphery that exhibit little volume change or expansion. Only during the final period of exhalation (points G to H), while the central regions are mostly unchanged, do these regions finally contract. Whereas ventilatory dissynchrony or pendelluft is a theoretical consequence of parallel mechanical inhomogeneity (59), particularly at high respiratory rates (2), these data may represent the first *in vivo* demonstration of this phenomenon in a subject during quiet breathing. Given that these regional expansion data may be obtained relatively easily in intact subjects, in three-dimensional distribution and with correlation to the high-resolution CT anatomic information, these approaches make it possible to define dynamic regional lung mechanical behavior to directly address indirectly measured phenomena such as pendelluft or serial and parallel ventilation inhomogeneities. Furthermore, it may be possible to apply these methods to detect early, localized disease processes that are physiologically silent until they become more widespread, such as fibrosis, emphysema, lung transplant rejection, or cystic fibrosis.

## IMAGE-BASED MODELING

Mathematical modeling of the respiratory system has been crucial to the development and advancement of a quantitative

understanding of lung physiology in general, and mechanics in particular (2, 60–62). This approach has become increasingly important with the explosion of information at the cellular and molecular levels, and the integration of quantitative models of physiology at multiple scales and for multiple organ systems is the goal of the International Union of Physiological Sciences Physiome Project (63, 64). In conjunction with that effort, M. Tawhai and associates at the University of Auckland (Auckland, New Zealand) have developed finite element models of the lung airways, vascular tree, and parenchymal mechanics that are based on individual subject anatomy determined from CT imaging (65–67). Figure 3 (p. 507) illustrates a deformable computer model of the sheep lung, built from CT images obtained at multiple inflation pressures and incorporating the actual airway tree, surface motion, and nonlinear parenchymal material properties (66). Data beyond the resolution of the CT images, such as small airways and alveoli, are modeled according to a volume-filling branching algorithm (65). Once built, the model generates predictions of lung deformation that can be compared with the actual volume and shape changes from the CT images. Over time, increasing complexity in terms of material properties, regional interdependence, and airflow phenomena, and eventually blood flow, gas exchange, and even cellular and molecular processes, will be incorporated as the modeling process moves toward the goals of the Physiome Project (63, 64).

## CONCLUSIONS

CT imaging opens a window into the dynamic distributed mechanical functioning of the respiratory system. Imaging has provided the data needed to refine our understanding of many aspects of the heterogeneous pathophysiology of the lung. Furthermore, our ability to measure and model airflow and regional lung mechanics is rapidly evolving, incorporating improving descriptions of lung material properties, interregional interactions, boundary conditions, and eventually gas exchange. Imaging contributes to this integration of structure and function in two important ways. CT image data are used to create actual anatomically accurate models, and functional imaging results (such as ventilation, perfusion, or regional mechanics) are used to test the model predictions and refine their design. In the near future, we may expect to see subject-specific image-based models of an individual patient's respiratory system, and we will begin to use these tools to first understand the evolution of pathologic processes and, ultimately, to predict the outcome of interventions such as surgery and to assess the progression of (subclinical) disease and response to therapy.

**Conflict of Interest Statement:** B.A.S. does not have a financial relationship with a commercial entity that has an interest in the subject of this manuscript. G.E.C. has received U.S. patent number 6,611,615, issued August 26, 2003, entitled Method and Apparatus for Generating Consistent Image Registration. This patent covers the general method of inverse consistent image registration. The patent was filed by the University of Iowa and is currently not licensed to anyone. D.A.L. does not have a financial relationship with a commercial entity that has an interest in the subject of this manuscript. J.M.R. does not have a financial relationship with a commercial entity that has an interest in the subject of this manuscript.

**Acknowledgment:** The authors thank Drs. Merryn Tawhai and Kelly Burrows (Bioengineering Institute, University of Auckland, Auckland, New Zealand; <http://www.bioeng.auckland.ac.nz/projects/lung/lung.php>) for providing the finite element lung mechanical model data used for Figure 3. The authors also thank Joo Hyun (Paul) Song, Wei Lu, Ph.D., and Parag J. Parikh, M.D., for work in generating the four-dimensional registration results shown in Figure 2.

## References

- Krogh A. The comparative physiology of respiratory mechanisms. Philadelphia, PA: University of Pennsylvania Press; 1941.
- Otis AB, McKerrow CB, Bartlett RA, Mead J, McIlroy MB, Selverstone NJ, Radford EP. Mechanical factors in distribution of pulmonary ventilation. *J Appl Physiol* 1956;8:427–442.
- Engel LA. Intraregional gas mixing and distribution. In: Engel LA, Paiva M, editors. Lung biology in health and disease, 1st ed.: Gas mixing and distribution in the lung. New York: Marcel Dekker; 1985. pp. 287–358.
- Hoppin FG Jr, Green M, Morgan MS. Relationship of central and peripheral airway resistance to lung volume in dogs. *J Appl Physiol* 1978;44:728–737.
- Macklem PT, Mead J. Resistance of central and peripheral airways measured by a retrograde catheter. *J Appl Physiol* 1967;22:395–401.
- Fredberg JJ, Ingram RH Jr, Castile RG, Glass GM, Drazen JM. Nonhomogeneity of lung response to inhaled histamine assessed with alveolar capsules. *J Appl Physiol* 1985;58:1914–1922.
- Chevalier PA, Rodarte JR, Harris LD. Regional lung expansion at total lung capacity in intact vs. excised canine lungs. *J Appl Physiol* 1978;45:363–369.
- Ball WC, Stewart PB, Newsham LGS, Bates DV. Regional pulmonary function studied with xenon-133. *J Clin Invest* 1962;41:519–531.
- Tajik JK, Tran BQ, Hoffman EA. New technique to quantitate regional pulmonary microvascular transit times from dynamic X-ray CT images. In: Hoffman EA, editor. Medical imaging 1998: physiology and function from multidimensional images. Proc. SPIE Vol. 3337. Bellingham, WA: International Society for Optical Engineering; 1998. pp. 24–32.
- Suga K. Technical and analytical advances in pulmonary ventilation SPECT with xenon-133 gas and Tc-99m-Technegas. *Ann Nucl Med* 2002;16:303–310.
- Murata K, Harumi I, Senda M, Todo G, Yonekura Y, Torizuka K. Ventilation imaging with positron emission tomography and nitrogen 13. *Radiology* 1986;158:303–307.
- Gur D, Drayer BP, Borovetz HS, Griffith BP, Hardesty RL, Wolfson SK. Dynamic computed tomography of the lung: regional ventilation measurements. *J Comput Assist Tomogr* 1979;3:749–753.
- Guenther D, Hanisch G, Kauczor HU. Functional MR imaging of pulmonary ventilation using hyperpolarized noble gases. *Acta Radiol* 2000;41:519–528.
- Bates JH, Lutchen KR. The interface between measurement and modeling of peripheral lung mechanics. *Respir Physiol Neurobiol* 2005;148:153–164.
- Parr DG, Stockley RA. Standardization of CT densitometry. *Radiology* 2004;230:887; author reply 887.
- Kemerink GJ, Lamers RJ, Thelissen GR, van Engelshoven JM. Scanner conformity in CT densitometry of the lungs. *Radiology* 1995;197:749–752.
- Bouhemad B, Richecoeur J, Lu Q, Malbouissin LM, Cluzel P, Roubey JJ. Effects of contrast material on computed tomographic measurements of lung volumes in patients with acute lung injury. *Crit Care* 2003;7:63–71.
- Gattinoni L, Presenti A, Torresin A, Baglioni S, Rivolta M, Rossi F, Scarani F, Marcolin R, Cappelletti G. Adult respiratory distress syndrome profiles by computed tomography. *J Thorac Imaging* 1986;1:25–30.
- Gattinoni L, Pesenti A, Avalli L, Rossi F, Bombino M. Pressure–volume curve of total respiratory system in acute respiratory failure: computed tomographic scan study. *Am Rev Respir Dis* 1987;136:730–736.
- Gattinoni L, Mascheroni D, Torresin A, Marcolin R, Fumagalli R, Vesconi S, Rossi GP, Rossi F, Baglioni S, Bassi F, et al. Morphological response to positive end expiratory pressure in acute respiratory failure: computerized tomography study. *Intensive Care Med* 1986;12:137–142.
- Gattinoni L, Caironi P, Pelosi P, Goodman LR. What has computed tomography taught us about the acute respiratory distress syndrome? *Am J Respir Crit Care Med* 2001;164:1701–1711.
- Bone RC. The ARDS lung: new insights from computed tomography [editorial]. *JAMA* 1993;269:2134–2135.
- Hubmayr RD. Perspective on lung injury and recruitment: a skeptical look at the opening and collapse story [critical care perspective]. *Am J Respir Crit Care Med* 2002;165:1647–1653.
- Li B, Christensen GE, Hoffman EA, McLennan G, Reinhardt JM. Establishing a normative atlas of the human lung: intersubject warping and registration of volumetric CT images. *Acad Radiol* 2003;10:255–265.
- Guerrero T, Sanders K, Noyola-Martinez J, Castillo E, Zhang Y, Tapia R, Guerra R, Borghero Y, Komaki R. Quantification of regional ventilation from treatment planning CT. *Int J Radiat Oncol Biol Phys* 2005;62:630–634.

26. Pan Y, Kumar D, Hoffman EA, Christensen GE, McLennan G, Song JH, Ross A, Simon BA, Reinhardt JM. Estimation of regional lung expansion via 3D image registration. *Proc. SPIE* 2005;5746:453–464.
27. Becker CR, Ohnesorge BM, Schoepf UJ, Reiser MF. Current development of cardiac imaging with multidetector-row CT. *Eur J Radiol* 2000;36:97–103.
28. Vedam SS, Keall PJ, Kini VR, Mostafavi H, Shukla HP, Mohan R. Acquiring a four-dimensional computed tomography dataset using an external respiratory signal. *Phys Med Biol* 2003;48:45–62.
29. Keall PJ, Starkschall G, Shukla H, Forster KM, Ortiz V, Stevens CW, Vedam SS, George R, Guerrero T, Mohan R. Acquiring 4D thoracic CT scans using a multislice helical method. *Phys Med Biol* 2004;49:2053–2067.
30. Chevrolet JC, Emrich J, Martin RR, Engel LA. Voluntary changes in ventilation distribution in the lateral posture. *Respir Physiol* 1979;38:313–323.
31. Brown RH, Herold CJ, Hirshman CA, Zerhouni EA, Mitzner W. *In vivo* measurements of airway reactivity using high-resolution computed tomography. *Am Rev Respir Dis* 1991;144:208–212.
32. Lu Q, Malbouissin LM, Mourgion E, Goldstein I, Coriat P, Rouby JJ. Assessment of PEEP-induced reopening of collapsed lung regions in acute lung injury: are one or three CT sections representative of the entire lung? *Intensive Care Med* 2001;27:1504–1510.
33. Vieira SR, Nieszowska A, Lu Q, Elman M, Sartorius A, Rouby JJ. Low spatial resolution computed tomography underestimates lung overinflation resulting from positive pressure ventilation. *Crit Care Med* 2005;33:741–749.
34. Puybasset L, Cluzel P, Chao N, Slutsky AS, Coriat P, Rouby J. A computed tomography scan assessment of regional lung volume in acute lung injury. *Am J Respir Crit Care Med* 1998;158:1644–1655.
35. Krell WS, Rodarte JR. Effects of chest wall on volume and strain patterns in canine lungs. *J Appl Physiol* 1985;58:1055–1060.
36. Rodarte JR, Hubmayr RD, Stamenovic D, Walters BJ. Regional lung strain in dogs during deflation from total lung capacity. *J Appl Physiol* 1985;58:164–172.
37. Hubmayr RD, Walters BJ, Chevalier PA, Rodarte JR, Olson LE. Topographical distribution of regional lung volume in anesthetized dogs. *J Appl Physiol* 1983;54:1048–1056.
38. Hubmayr RD, Hill MJ, Wilson TA. Nonuniform expansion of constricted dog lungs. *J Appl Physiol* 1996;80:522–530.
39. Sprung J, Deschamps C, Hubmayr RD, Walters BJ, Rodarte JR. *In vivo* regional diaphragm function in dogs. *J Appl Physiol* 1989;67:655–662.
40. Martynowicz MA, Walters BJ, Hubmayr RD. Mechanisms of recruitment in oleic acid-injured lungs. *J Appl Physiol* 2001;90:1744–1753.
41. Martynowicz MA, Minor TA, Walters BJ, Hubmayr RD. Regional expansion of oleic acid-injured lungs. *Am J Respir Crit Care Med* 1999;160:250–258.
42. Ritman EL, Kinsey JH, Robb RA, Gilbert BK, Harris LD, Wood EH. Three-dimensional imaging of heart, lungs, and circulation. *Science* 1980;210:273–280.
43. Hoffman EA, Sinak LJ, Robb RA, Ritman EL. Noninvasive quantitative imaging of shape and volume of lungs. *J Appl Physiol* 1983;54:1414–1421.
44. Hoffman EA, Ritman EL. Effect of body orientation on regional lung expansion in dog and sloth. *J Appl Physiol* 1985;59:481–491.
45. Rouby JJ, Puybasset L, Nieszowska A, Lu Q. Acute respiratory distress syndrome: lessons from computed tomography of the whole lung. *Crit Care Med* 2003;31:S285–S295.
46. Gattinoni L, Pelosi P, Suter PM, Pedoto A, Vercesi P, Lissoni A. Acute respiratory distress syndrome caused by pulmonary and extrapulmonary disease: different syndromes? *Am J Respir Crit Care Med* 1998;158:3–11.
47. Pelosi P, D'Onofrio D, Chiumello D, Paolo S, Chiara G, Capelozzi VL, Barbas CS, Chiaranda M, Gattinoni L. Pulmonary and extrapulmonary acute respiratory distress syndrome are different. *Eur Respir J Suppl* 2003;42:48s–56s.
48. Vieira SRR, Puybasset L, Lu Q, Richecoeur J, Cluzel P, Coriat P, Rouby J. A scanographic assessment of pulmonary morphology in acute lung injury. *Am J Respir Crit Care Med* 1999;159:1612–1623.
49. Vieira SR, Puybasset L, Richecoeur J, Lu Q, Cluzel P, Gusman PB, Coriat P, Rouby JJ. A lung computed tomographic assessment of positive end-expiratory pressure-induced lung overdistension. *Am J Respir Crit Care Med* 1998;158:1571–1577.
50. Toga AW, editor. Brain warping. San Diego, CA: Academic Press; 1999.
51. Horn BKP, Schunck BG. Determining optical flow. *Artif Intell* 1981;17:185–203.
52. Dougherty L, Asmuth JC, Gefter WB. Alignment of CT lung volumes with an optical flow method. *Acad Radiol* 2003;10:249–254.
53. Guerrero T, Zhang G, Huang TC, Lin KP. Intrathoracic tumour motion estimation from CT imaging using the 3D optical flow method. *Phys Med Biol* 2004;49:4147–4161.
54. Coselman MM, Balter JM, McShan DL, Kessler ML. Mutual information based CT registration of the lung at exhale and inhale breathing states using thin-plate splines. *Med Phys* 2004;31:2942–2948.
55. Krishnan S, Beck KC, Reinhardt JM, Carlson KA, Simon BA, Albert RK, Hoffman EA. Regional lung ventilation from volumetric CT scans using image warping functions. Presented at the International Symposium on Biomedical Imaging, Washington, DC, April 15–18, 2004.
56. Christensen GE. Consistent linear-elastic transformations for image matching. In: Kuba A, Samal M, Todd-Pokropek A, editors. Lecture notes in computer science. Vol. 1613: Proc. 16th Int. Conf. on Information Processing in Medical Imaging (IPMI '99), Visegrad, Hungary, June 28–July 2, 1999. Berlin: Springer-Verlag; 1999. pp. 224–237.
57. Johnson HJ, Christensen GE. Consistent landmark and intensity-based image registration. *IEEE Trans Med Imaging* 2002;21:450–461.
58. Christensen GE, Johnson HJ. Consistent image registration. *IEEE Trans Med Imaging* 2001;20:568–582.
59. Safonoff I, Emmanuel GE. The effect of Pendelluft and dead space on nitrogen clearance: mathematical and experimental models and their application to the study of the distribution of ventilation. *J Clin Invest* 1967;46:1683–1693.
60. Takishima T, Mead J. Tests of a model of pulmonary elasticity. *J Appl Physiol* 1972;33:576–581.
61. Permutt S, Riley RL. Hemodynamics of collapsible vessels with tone: the vascular waterfall. *J Appl Physiol* 1963;18:924–932.
62. Venegas JG, Tsuzaki K, Fox BJ, Simon BA, Hales CA. Regional coupling between chest wall and lung expansion during HFV: a positron imaging study. *J Appl Physiol* 1993;74:2242–2252.
63. Crampin EJ, Halstead M, Hunter P, Nielsen P, Noble D, Smith N, Tawhai M. Computational physiology and the Physiome Project. *Exp Physiol* 2004;89:1–26.
64. Hunter P, Smith N, Fernandez J, Tawhai M. Integration from proteins to organs: the IUPS Physiome Project. *Mech Ageing Dev* 2005;126:187–192.
65. Tawhai MH, Hunter P, Tschirren J, Reinhardt J, McLennan G, Hoffman EA. CT-based geometry analysis and finite element models of the human and ovine bronchial tree. *J Appl Physiol* 2004;97:2310–2321.
66. Tawhai MH, Nash MP, Tschirren J, Hoffman EA, Hunter PJ. An image-based computational model of ovine lung mechanics and ventilation distribution. *Proc. SPIE* 2005;5746:84–91.
67. Burrowes KS, Hunter PJ, Tawhai MH. Anatomically based finite element models of the human pulmonary arterial and venous trees including supernumerary vessels. *J Appl Physiol* 2005;99:731–738.

COMPUTED TOMOGRAPHY STUDIES OF LUNG VENTILATION AND PERFUSION

Eric A. Hoffman and Deekiee Chon (pages 492–498)

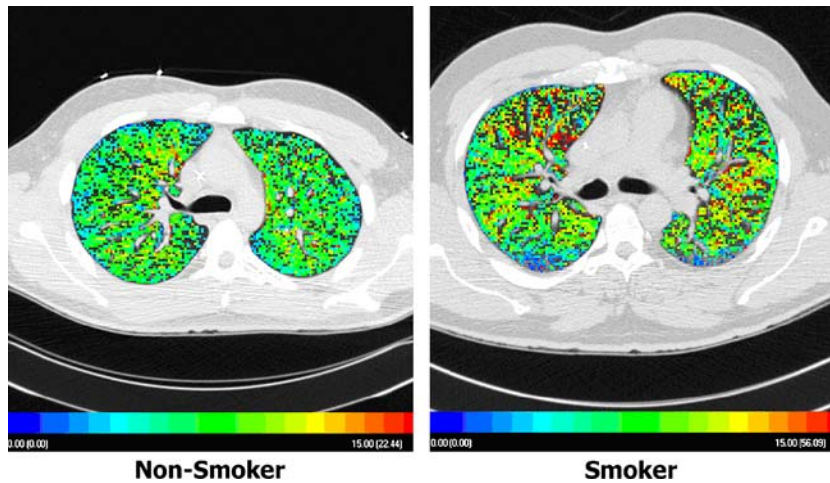


Figure 2. Color maps of regional pulmonary blood flow in nonsmoking and smoking subjects. Note the increased heterogeneity of flow in the smoker, presumably indicating the results of inflammatory processes. The color scales under each image range from 0 to 15 ml/min/g.

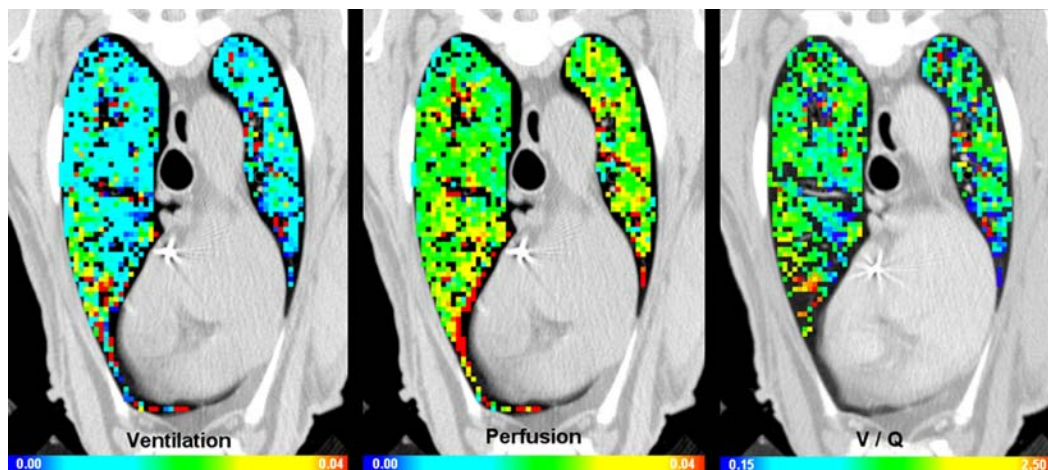


Figure 3. Color maps of regional specific ventilation (left), regional perfusion (middle), and regional  $\dot{V}/\dot{Q}$  (right) in a prone sheep. Because of the simultaneously derived anatomic detail via CT, we are able to express ventilation and perfusion through normalization to air, tissue, or blood content of the region. To achieve a measure of regional specific ventilation, one would normalize the measures of ventilation to regional air content. However, here we simply express ventilation and perfusion as a function of voxel volume because  $\dot{V}/\dot{Q}$  provides self-normalization.

COMPUTED TOMOGRAPHY STUDIES OF LUNG MECHANICS

Brett A. Simon, Gary E. Christensen, Daniel A. Low, and Joseph M. Reinhardt (pages 517–521)

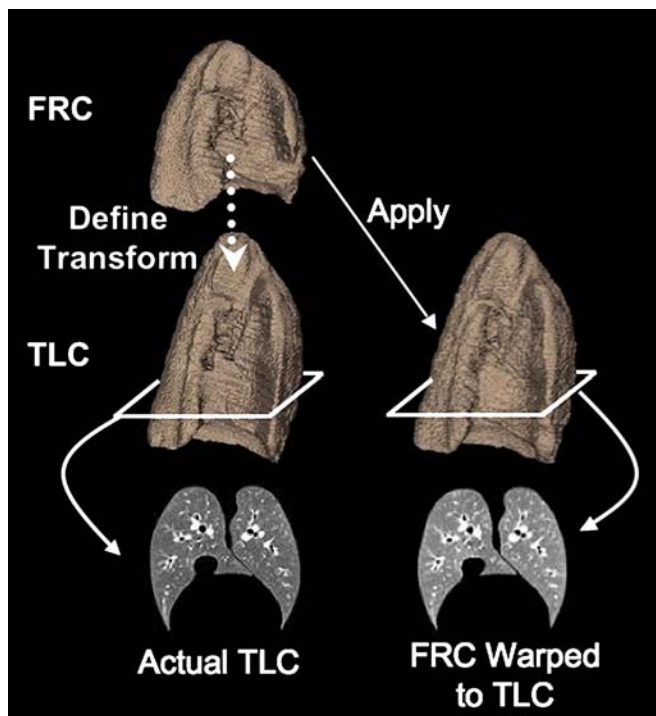
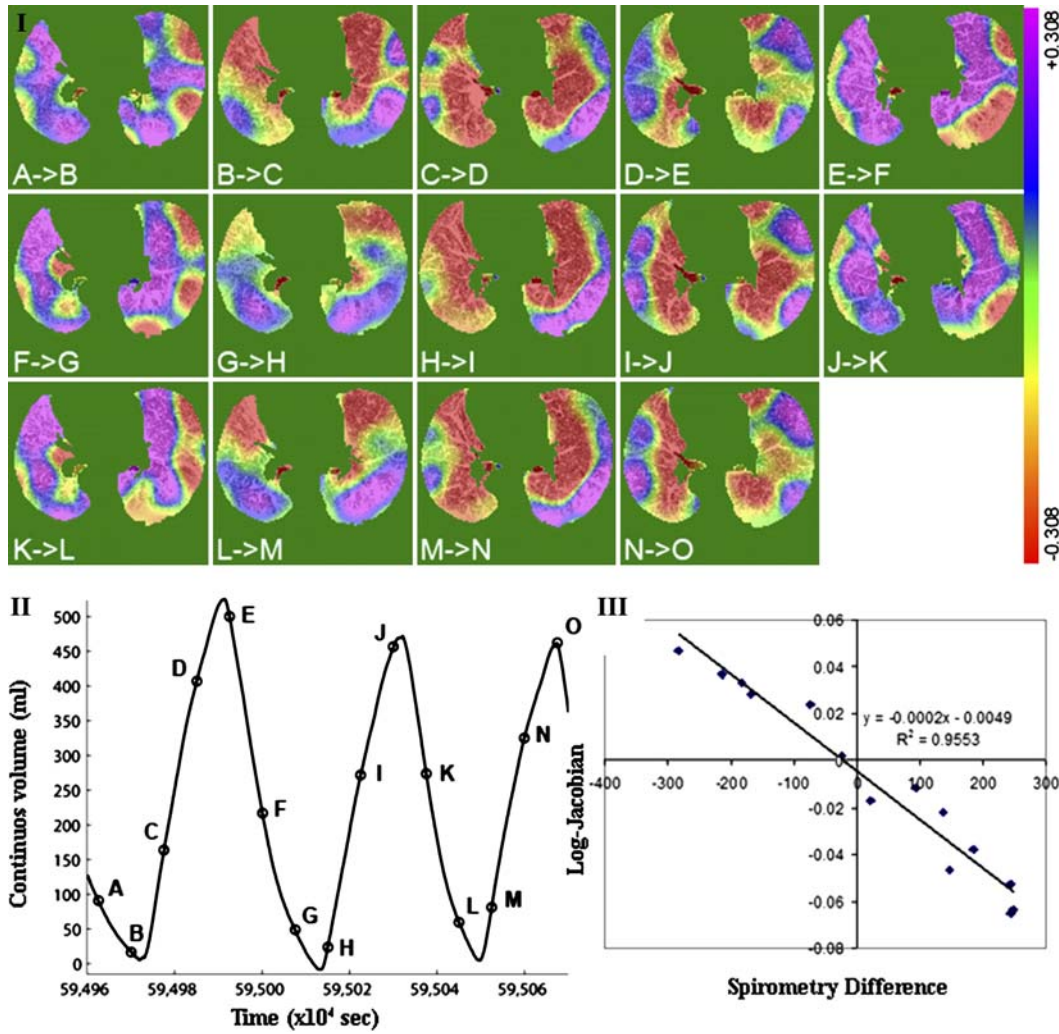
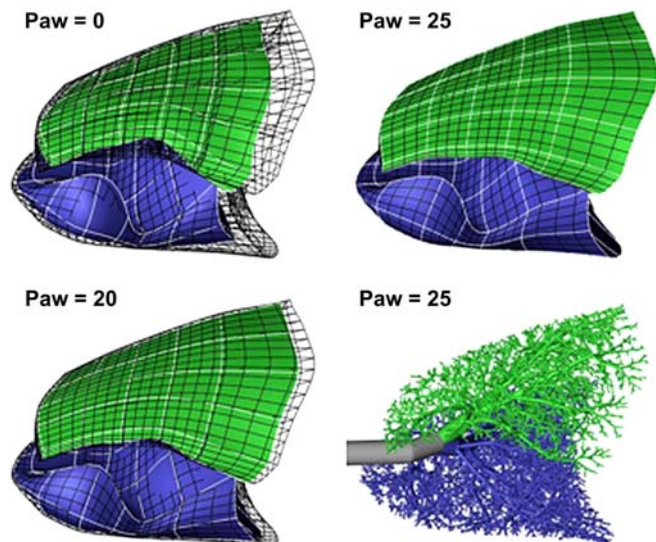


Figure 1. Example of the image registration process, in which a human lung computed tomography (CT) image at functional residual capacity (FRC) is mapped to total lung capacity (TLC). The mathematical transform defined is applied to the FRC image, and the original TLC slice is seen to closely resemble the corresponding “warped” FRC slice.



**Figure 2.** Color-coded log-Jacobian (quantitative regional expansion or contraction) images superimposed on the target CT volume for 15 images obtained from a human subject during three spontaneous breaths. *I*: log-Jacobian superimposed on the CT slice for each of the 14 image registrations. The subscripts for each panel correspond to the points in the respiratory cycle (*II*) at which the image pairs were obtained. *Magenta* corresponds to a contraction, *red* corresponds to an expansion, and *green* corresponds to no change. *III*: Correlation between the average log-Jacobian and the volume changes measured by spirometry.



**Figure 3.** Image-based computational model of sheep lung mechanics (66). Finite element meshes of a sheep lung at distending pressures of 0, 20, and 25 cm H<sub>2</sub>O demonstrate simulated deformation from 25 cm H<sub>2</sub>O (wireframe mesh). Also shown are the CT-based airway tree and generated volume-filling small airways (at 25 cm H<sub>2</sub>O; *bottom right*) embedded within the finite element mesh. Figure reprinted by permission from M. Tawhai (University of Auckland, Auckland, New Zealand). Paw = airway pressure.